Polymer Chemistry

ROYAL SOCIETY OF CHEMISTRY

PAPER

View Article Online
View Journal

Check for updates

Cite this: DOI: 10.1039/d6py00172f

Creep-resistant, extrudable, and recyclable polyolefin covalent adaptable networks incorporating azine cross-links *via* reactive processing

Mathew J. Suazo,[a] Stephanie M. Barbon,[b] Hayley A. Brown,[c] Evelyn Auyeung,[c] Colin Li Pi Shan[c] and John M. Torkelson *[a,d]

Polyolefins, encompassing polymers such as polyethylene (PE) and ethylene-based copolymers, are the world's most widely produced class of plastics due to their versatility and facile property tunability. Although these materials are recyclable, in practice their recycling rates are low due to a range of issues, including thermomechanical degradation. Furthermore, converting polyolefins into thermosets, such as PEX (made by cross-linking PE to form a permanent network), may yield property improvements but it comes at the cost of reprocessability and, thus, recyclability. The development of covalent adaptable networks (CANs), which utilize dynamic rather than static cross-links, has provided a promising avenue for improving the sustainability of polyolefin-based materials. By incorporating dynamic covalent bonds (associative or dissociative in nature) into polyolefin precursor materials, the resulting polyolefin CANs may exhibit improved properties and full recovery of these properties upon recycling. Here, we used radical-based reactive processing to introduce associative azine dynamic cross-links into a variety of ethylene-based polymers, yielding robust, reprocessable CANs. By reacting various PEs and ethylene/1-octene copolymers with 0.6 wt% dicumyl peroxide and 5 wt% bis(4-methacryloyloxybenzylidene) hydrazine (BiBeN methacrylate, BBMA), we obtained CANs that exhibited full recovery of cross-link density and thermomechanical properties after multiple cycles of remolding, as well as substantial, elevated-temperature creep resistance and amenability to industrially relevant processing methods (*e.g.*, injection molding and extrusion). Finally, compared with our previous studies using aromatic-disulfide-based and dialkylamine-disulfide-based cross-linkers, our BBMA-based polyolefin CANs exhibited improved cross-link density and elevated-temperature creep suppression, required less radical initiator, and were reprocessable at lower temperature.

Received 21st February 2026,
Accepted 20th April 2026

DOI: 10.1039/d6py00172f

rsc.li/polymers

Open Access Article. Published on 01 mayo 2026. Downloaded on 26/5/2026 06:12:29.
This article is licensed under a Creative Commons Attribution 3.0 Unported Licence.

1. Introduction

As the world's most-produced plastic, polyethylene (PE) exhibits significant versatility and property tunability which makes it well-suited to a variety of applications.[1–3] Variations in the polymerization method used to synthesize PE can result in low-density or high-density PE (LDPE or HDPE), which differ significantly in properties such as crystallinity and dispersity. Variations in synthesis conditions can further tailor properties such as molecular weight.[1,4] The copolymerization of ethylene with α-olefins provides another route for property tuning. Linear low-density PE (LLDPE) may be produced by utilizing a small proportion of α-olefin (typically 10% or lower) to yield a material with both low dispersity and increased short-chain branching, which stands in contrast to conventional LDPE and HDPE.[1,4] Meanwhile, incorporating higher proportions of α-olefin comonomer allows for the production of specialty plastics which may access a wider variety of microstructures and performance metrics; for instance, random and multiblock ethylene/1-octene copolymers (r-EOC and OBC, respectively) are commercially produced for such purposes.[5–7]

Although avenues exist for recycling thermoplastic materials such as PE (due to their moldability at high temperatures), the reduction in properties that often results from thermomechanical degradation during reprocessing means that plastic recycling rates have remained below 10% worldwide from year to year.[2,8] An additional challenge arises from the

[a]*Department of Materials Science and Engineering, Northwestern University, Evanston, IL 60208, USA. E-mail: j-torkelson@northwestern.edu*
[b]*The Dow Chemical Company, Midland, MI 48674, USA*
[c]*The Dow Chemical Company, Lake Jackson, TX 77566, USA*
[d]*Department of Chemical and Biological Engineering, Northwestern University, Evanston, IL 60208, USA*

Open Access Article. Published on 01 mayo 2026. Downloaded on 26/5/2026 06:12:29.
This article is licensed under a Creative Commons Attribution 3.0 Unported Licence.

production of thermosets such as cross-linked PE (PEX); the conventional methods of thermoset synthesis, such as reactive extrusion, result in the formation of permanent cross-links between the constitutive chains of the precursor material and thus a permanent network structure.[9–12] While these permanent cross-links provide robust mechanical properties and chemical resistance to the thermoset material (making it suitable for applications such as pipework or cable insulation), this comes at the expense of recyclability, as the material will simply degrade rather than melt and flow with increasing temperature.[9–12] Therefore, sustainability challenges remain to be addressed for PE, PEX, and other commercially produced thermoplastic and thermoset materials.

A promising avenue for producing materials with robust properties under use conditions and full recyclability under processing conditions is the incorporation of dynamic covalent cross-links.[3,12–25] In contrast to permanent cross-links, which remain static until degradation occurs, dynamic cross-links may rearrange in response to a stimulus (heat, light, pressure, *etc.*), enabling network reconfiguration and thus reprocessability of the material as a whole.[14–17] Network polymers incorporating dynamic covalent cross-links are often referred to as covalent adaptable networks (CANs); the chemistries of the dynamic cross-links are typically classified as dissociative or associative.[14,17,18,21] CANs containing dissociative cross-links experience a reduction in cross-link density while the dynamic chemistry is active, as the functional groups of the cross-links must fully decouple before seeking out new partners to recombine and recover the network structure.[13,20] In contrast, under normal conditions for characterizing cross-link density, CANs containing strictly associative cross-links (sometimes referred to as vitrimers[16,19,22]) exhibit a constant cross-link density with active dynamic chemistry due to the simultaneous breakage and reformation of the cross-links.[15,16,19] In addition, some CANs exhibit characteristics of both dissociative and associative dynamic chemistries.[26–29]

Given the ability of existing thermoset production routes to incorporate dynamic rather than static cross-links, numerous studies have successfully synthesized polyolefin CANs using various dynamic chemistries in recent years.[3,11,12,30–50] In 2022,[38] our group pioneered a simple, one-step method using radical-based reactive processing to produce fully reprocessable CANs from virgin and waste LDPE and HDPE (in contrast to previous studies that required external catalysis, prefunctionalized PEs, and other complicating factors[30–37]). Our subsequent studies extended this approach to the production of r-EOC[39] and OBC[42] CANs, in each case utilizing BiTEMPS methacrylate (BTMA; a cross-linker containing a dialkylamine disulfide dynamic bond that undergoes dissociative-type exchange when active[51–54]) to graft dynamic cross-links between constituent chains of the precursor polyolefins.[38,39,42] In doing so, we demonstrated the applicability of our radical-based reactive process to a range of precursor materials (with our recent study grafting BTMA to ethylene-vinyl acetate copolymers extending this finding to materials beyond pure polyolefins[55]), as well as providing insight into the structure–property relationships, self-healability, and extrudability of the resulting CANs.[38,39,41,42]

Furthermore, our development of BiPheS methacrylate (BPMA; a cross-linker containing an aromatic disulfide bond that undergoes a [2 + 1] radical-mediated exchange and exhibits both associative and dissociative characteristics when active[56–58]) and our proof-of-concept study[58] copolymerizing it with *n*-hexyl methacrylate (HMA) led us to hypothesize that BPMA could impart improved high-temperature performance to polyolefin CANs. Indeed, by reactively processing BPMA with a range of PEs as well as an r-EOC and an OBC,[44] we demonstrated a significant improvement in high-temperature creep resistance compared to similar CANs made with BTMA while also enabling full property recovery at extrusion temperatures as high as 260 °C (60 °C higher than previously demonstrated using BTMA[39]). Additionally, we recently showed that introducing additional aromatic rings into the BPMA structure and/or using vinyl aromatic additives enabled the first production of CANs from polypropylene (PP)[47,48] and propylene-ethylene copolymers (PEC),[49] owing to the ability of the aromatic groups to provide resonance stabilization of radicals, thereby suppressing the β-scission of propylene repeat units that occurs upon exposure to radicals.[47–49,59] The resulting PP and PEC CANs exhibited facile extrudability and full property recovery upon reprocessing, further demonstrating the utility of aromatic disulfide dynamic bonds in producing robust CANs from a variety of precursor materials.[44,47–49]

Recently, we were the first to demonstrate the incorporation of azine dynamic bonds into a CAN by radical-based methods,[60] enabled by our development of BiBeN methacrylate (BBMA; a cross-linker containing an azine bond that undergoes associative-type [2 + 2] metathesis when active[60,61]). Azines had previously seen little exploration in the CAN literature, and the few prior studies employed methods not readily applicable to commercial polymer network manufacturing.[62–66] Our success in producing HMA–BBMA copolymer CANs by free-radical copolymerization[60] also enabled us to compare their properties and performance with those of our previously-studied HMA–BPMA copolymer CANs.[58] For instance, with the same molar proportion of added cross-linker, the HMA–BBMA copolymer exhibited a 36% increase in cross-link density compared to its HMA–BPMA counterpart, highlighting BBMA's greater efficiency in introducing effective cross-links into a network.[58,60] The HMA–BBMA copolymer also showed an 8-fold reduction in elevated-temperature creep compared to the HMA–BPMA copolymer (at 210 °C) and accommodated a much lower reprocessing temperature (120 °C) for recovery of the equilibrium cross-link density (*vs.* 200 °C for HMA–BPMA).[58,60] In the current study, we were motivated to apply BBMA to produce reactively processed polyolefin CANs, as our group had previously done this extension from copolymer CANs to reactively processed CANs for BTMA and BPMA.[38,39,42,44] In doing so, we would be able to examine any distinctions in polyolefin CAN behavior resulting from our use of the novel BBMA chemistry; this is important given the major differences evident in the elevated-temperature stress

This journal is © The Royal Society of Chemistry 2026

Open Access Article. Published on 01 mayo 2026. Downloaded on 26/5/2026 06:12:29.
This article is licensed under a Creative Commons Attribution 3.0 Unported Licence.

relaxation dynamics of HMA-based CANs made with the BBMA cross-linker (which undergoes [2 + 2] metathesis) *vs.* BPMA (which undergoes [2 + 1] exchange) and BTMA (which undergoes dissociation).[52,58,60] In particular, we anticipated that BBMA would enable facile (re)processability at more moderate temperatures than BPMA while improving cross-link incorporation and suppressing high-temperature creep.

Here, we synthesized BBMA-based polyolefin CANs from precursor polymers (LDPE, LLDPE, HDPE, r-EOC, and OBC) *via* radical-based reactive processing. After determining an approximately optimal loading of dynamic cross-linker and radical initiator, we verified robust network formation across our CANs and confirmed full property recovery (and thus reprocessability) over multiple compression-molding cycles. We also compared various properties with those of our previous BPMA-based polyolefin CANs and, for elevated-temperature creep resistance, with BTMA-based CANs.[44] Finally, we assessed the amenability of our BBMA-based CANs to industrially relevant (re)processing methods, including injection molding and extrusion. In total, we validated the suitability of BBMA for producing robust, creep-resistant, and recyclable polyolefin CANs, providing a favorable route to replace commercial thermosets with dynamic polymer networks.

2. Experimental

2.1. Materials

All chemicals were used as received unless otherwise stated. All precursor polyolefins (LDPE, HDPE, LLDPE, r-EOC, and OBC) were from The Dow Chemical Company; the manufacturer provided densities and melt flow indices. 4,4′-Dihydroxybenzalazine (95%) was purchased from 10X Chem. Methacryloyl chloride (97%), triethylamine (99%), *N*,*N*-dimethylacetamide (DMAc, anhydrous, 99.8%), dicumyl peroxide (DCP, 98%), *o*-xylene (98%), potassium carbonate (99.0%), and magnesium sulfate (99.5%) were purchased from Sigma-Aldrich. Sodium chloride (99.5%), dichloromethane (99.5%), chloroform (99.8%), and methanol (99.8%) were purchased from Fisher Scientific. DMAc was dried over activated 4 Å molecular sieves for at least 48 h before use.

2.2. Synthesis of bis(4-methacryloyloxybenzylidene)hydrazine (BiBeN methacrylate, BBMA) cross-linker

Bis(4-methacryloyloxybenzylidene)hydrazine (BiBeN methacrylate, BBMA) was synthesized by following a literature procedure.[60] ^{1}H NMR (500 MHz, $CDCl_3$): δ 8.86 (d, J = 3.8 Hz, 2H), 8.05–7.93 (m, 4H), 7.33–7.28 (m, 4H), 6.41 (q, J = 1.1 Hz, 2H), 5.83 (dp, J = 5.9, 1.5 Hz, 2H), 2.10 (q, J = 1.5 Hz, 6H). Hi-Res MS (ESI): m/z found [M–H$^+$] for [$C_{22}H_{20}O_4N_2$–H$^+$] 377.30 (calcd 377.42).

2.3. Chemical characterization of BBMA

BBMA was characterized using methods described in the literature.[60] ^{1}H nuclear magnetic resonance (NMR) spectroscopy was conducted using a Bruker Avance III 500 MHz NMR spectrometer. Measurements were taken at room temperature with deuterated chloroform as the solvent. Electrospray ionization (ESI) mass spectrometry (MS) was conducted using a Bruker AmaZon-SL configured with an Agilent 1100 Series high-performance liquid chromatography module, an ESI source, and a 3D ion trap mass analyzer. Measurements employed a mobile phase composition of 20% methanol/80% dichloromethane and collected the positive-ion spectra.

2.4. Synthesis of polyolefin CANs

Typically, pellets of a selected polyolefin (LDPE, HDPE, LLDPE, r-EOC, or OBC) (0.5 to 2.0 g basis) were added to an Atlas Laboratory Mixing Molder (flushed twice with the selected polyolefin before synthesis). Unless stated otherwise, 5 wt% BBMA and 0.6 wt% DCP (both in powder form) were added to the mixer along with two or three steel balls to emulate the chaotic mixing of reactive extrusion and promote homogenization.[67] The weight percentages of BBMA and DCP were calculated relative to the mass of polyolefin added to the mixer. The blends were homogenized at 120 rpm for 3 to 5 min at a temperature depending on the polyolefin used (120 °C for r-EOC, 130 °C for LDPE, LLDPE, and OBC, and 140 °C for HDPE). While the mixer's rotor remained at constant angular velocity, the mixer's cup was periodically manually cranked up and down to aid the blending process. The uncured blends were then removed from the mixer with a spatula and compression-molded at 160 °C using a PHI press (model 0230C-X1) with a 10-ton (~8 MPa) ram force for 1.0 h, yielding cured 1st-molded films (~0.6 mm thick).

2.5. Reprocessing of CANs *via* compression molding

Unless otherwise stated, 1st-molded CAN films were cut into mm-sized pieces and compression molded at 160 °C using a PHI press (model 0230C-X1) with a 10-ton (~8 MPa) ram force for 1.0 h, yielding 2nd-molded films. This process was then repeated, starting with 2nd-molded films to yield 3rd-molded films.

2.6. Reprocessing of CANs *via* injection molding and extrusion

r-EOC CANs (~5 g) containing 5 wt% BBMA and 0.6 wt% DCP were cut into pieces and fed into an extruder (HAAKE MiniLab 3, Thermo Scientific) set to 30 rpm and 160 °C. The molten sample was then continuously cycled through the extruder for an estimated residence time of 5 min. It was then either retrieved from the cycling channel (yielding an injection-molded sample) or extruded through the outlet (yielding an extruded sample).

2.7. Radical activity studies

To assess the possibility of cross-linker homopolymerization, 50 mg BBMA and 6 mg DCP were dissolved in 1.0 mL *o*-xylene and heated at 140 °C for 12 h.[47] To assess the potential susceptibility of the azine motif to radical exposure, 50 mg 4,4′-dihydroxybenzalazine and 6 mg DCP were dissolved in 1.0 mL DMAc and heated at 140 °C for 12 h.

Open Access Article. Published on 01 mayo 2026. Downloaded on 26/5/2026 06:12:29.
This article is licensed under a Creative Commons Attribution 3.0 Unported Licence.

2.8. Differential scanning calorimetry (DSC)

Measurements were performed on ~5 mg samples of the CANs in hermetically sealed aluminum pans under nitrogen flow using a TA Instruments DSC250. The following cycle was applied twice to each sample: (1) heating to 180 °C at a rate of 10 °C min^{-1}, (2) holding at 180 °C for 5 min, and (3) cooling to 0 °C at a rate of 10 °C min^{-1}, yielding a heat flow (W g^{-1}) *vs.* temperature plot. The melting peak and endpoint temperatures ($T_{m,peak}$ and $T_{m,endpoint}$, respectively) were determined from the endothermic peak of the second heating scan. Percent crystallinity was determined by integrating the crystallization peak of the second cooling scan to obtain the sample's latent heat of fusion, which was then divided by the latent heat of fusion for fully crystalline PE (293 J g^{-1}).[68]

2.9. Thermogravimetric analysis (TGA)

Measurements were performed using a Mettler Toledo TGA/DSC3+ on CAN samples in alumina pans under a combined gas flow of 70 mL min^{-1} (20 mL min^{-1} nitrogen, 50 mL min^{-1} air). Each sample was initially held at 50 °C for 5 min, then heated to 600 °C at 10 °C min^{-1}. The degradation temperature (T_d) of each sample was taken as the temperature at which the sample reached a 5% mass loss.

2.10. Gel content determination

Small pieces of each CAN (with mass m_o) were immersed in *o*-xylene (~1 mL mg^{-1}) at 120 °C for 18 h, after which the pieces had swelled in the solvent. The pieces were then retrieved and dried in a vacuum oven for 48 h before being weighed (m_d). Gel content was determined from triplicate measurements as follows: gel content (%) = $100(m_d/m_o)$.

2.11. Dynamic mechanical analysis (DMA)

Tension-mode, small-amplitude oscillatory DMA temperature ramps and frequency sweeps were performed on samples using a TA Instruments RSA-G2 Solids Analyzer. Storage modulus (E'), loss modulus (E''), and damping ratio (tan $\delta = E''/E'$) were recorded as functions of temperature. Unless otherwise stated, temperature ramps were performed under airflow at a heating rate of 3 °C min^{-1}, a frequency of 1.0 Hz, and an oscillatory strain of 0.03%, and frequency sweeps were conducted under airflow from 10.0 to 0.01 rad s^{-1} at 170 °C using an oscillatory strain of 1.0%.

2.12. Creep

Shear-mode creep experiments were performed by applying a 3.0 kPa stress to sample discs cut from 1st-molded films of CANs containing 5 wt% BBMA and 0.6 wt% DCP as well as precursor polyolefins (~0.6 mm thick, ~8 mm in diameter). Measurements were conducted using an Anton-Paar MCR 302e rheometer with an oven-hood attachment and an 8 mm parallel-plate fixture. Samples were equilibrated at 150 °C for 10 min under 2.0 N of applied normal force, after which creep tests of varying duration were conducted (10 000 s for CANs, 200 s for precursor polyolefins). The viscous creep strain of a CAN was calculated by extrapolating the slope of the best-fit line through the data between t = 9000 s and t = 10 000 s (the observed linear portion of the curve) back to t = 0 s and subtracting this y-intercept from the final strain value at t = 10 000 s. The viscous creep strain of a precursor polyolefin was taken as the final strain at t = 200 s.

2.13. Stress relaxation

Tension-mode stress relaxation experiments were conducted on CAN samples using a TA Instruments RSA-G2 Solids Analyzer. Samples were thermally equilibrated at the test temperature for 10 min before testing. An instantaneous 3% strain was held constant over the course of the experiment, and the stress relaxation modulus ($E(t)$) for each sample was monitored as a function of time. Experiments were run until each sample had relaxed at least 80% of its initial stress (*i.e.*, $E(t)/E_0 < 0.20$).

3. Results and discussion

3.1. Standard formulation for reactively processed BBMA-based CANs

We first sought a formulation that would enable the successful synthesis of reprocessable CANs from our range of precursor materials, including low-density, linear low-density, and high-density polyethylene (LDPE, LLDPE, and HDPE, respectively) as well as random and multi-block ethylene/1-octene copolymers (r-EOC and OBC, respectively). Scheme 1 illustrates our procedure for converting neat polyolefins into CANs by reactive processing, and Tables 1 and S1 provide relevant properties of the neat polyolefins we employed.[44,69–73] In a typical synthesis, we used a benchtop melt-mixer to blend 0.5–2.0 g of a polyolefin with 5 wt% (relative to the polyolefin mass) of our BiBeN methacrylate (BBMA) cross-linker and 0.6 wt% dicumyl peroxide (DCP) as a radical initiator. The blend was mixed for 3–5 min at 120 rpm and 120 °C for the r-EOC, 130 °C for the LDPE, LLDPE, and OBC, or 140 °C for the HDPE (depending on the endpoint melting temperature, $T_{m,endpoint}$, of each polyolefin, but low enough to avoid significant radical initiation by DCP). Following this, the homogenized blend was removed from the mixer and compression-molded at 160 °C and 8 MPa

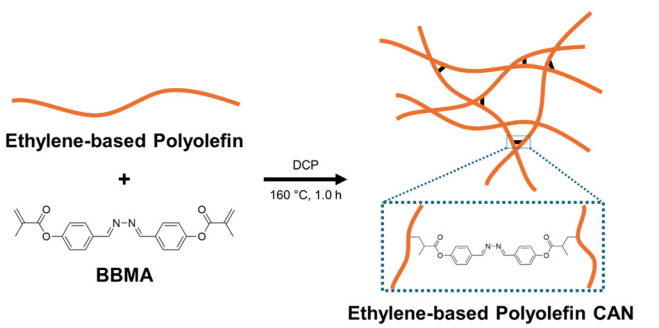

Scheme 1 Synthesis of a CAN from an ethylene-based polyolefin (polyethylene, ethylene–octene copolymer), BiBeN methacrylate (BBMA), and dicumyl peroxide (DCP) *via* reactive processing at 160 °C.

This journal is © The Royal Society of Chemistry 2026

Open Access Article. Published on 01 mayo 2026. Downloaded on 26/5/2026 06:12:29.
This article is licensed under a Creative Commons Attribution 3.0 Unported Licence.

Table 1 Properties of neat precursor polymers

Material	Crystallinity[a] (%)	$T_{m,peak}$ [a] (°C)	$T_{m,endpoint}$ [a] (°C)	Density[b] (g cm^{-3})	Melt flow index[b,c] (g per 10 min)	M_w (kg mol^{-1})	$Đ$	1-Octene content (wt%)
LDPE	43	112	121	0.924	4.2	80[d]	7.3[d]	0[b]
LLDPE	50	123	132	0.920	1.0	110[e]	3.7[e]	10[e]
HDPE	70	130	142	0.953	0.38	115[f]	3.0[f]	0[b]
r-EOC	18	63	85	0.870	1.0	120[g]	2.0[g]	38[b]
OBC	16	122	132	0.877	1.0	130[h]	2.6[h]	39[h]

[a] Ref. 44. [b] Data provided by manufacturer. [c] Collected at 190 °C using 2.16 kg load. [d] Ref. 69. [e] Ref. 70. [f] Ref. 71. [g] Ref. 72. [h] Ref. 73.

for 1.0 h, yielding a 1st-molded, cross-linked CAN as depicted in Scheme 1. This procedure has previously been shown to produce homogeneous blends[67] and, subsequently, polyolefin CANs without macroscopic or nanoscale phase separation.[38]

As previously demonstrated,[38,39,42,44] this reactive processing procedure is enabled using a bifunctional dynamic cross-linker with methacrylate end groups such as BBMA. At high temperatures, the peroxide bond of DCP cleaves to form free radicals, which then abstract hydrogen atoms from the polyolefin chains, forming macroradicals on the chains. These macroradicals then react with the double bonds of the methacrylate end groups of the dynamic cross-linkers, thereby grafting the cross-linkers to the polyolefin chains. Dynamic cross-links are thus obtained when both ends of a cross-linker molecule are grafted to different polyolefin chains; see Scheme 1. We note the possibility of side reactions during this procedure that can result in permanent cross-links (*e.g.*, *via* the reaction of two macroradicals directly and permanently linking two chains) or dynamic bonds that do not contribute to the network structure (*e.g.*, a dangling end left ungrafted when only one side of the cross-linker reacts with a chain macroradical, or both ends of a cross-linker reacting with the same chain to form a loop).[38,44] Therefore, we sought to determine a cross-linker/radical initiator loading that would minimize the formation of permanent cross-links (to maintain reprocessability) while still yielding a robust, dynamically cross-linked network structure.

Furthermore, we sought to examine the potential distinctions arising from the use of BBMA's azine dynamic chemistry. Azine exchange, representing a [2 + 2] metathesis and thus a fully associative dynamic chemistry,[60,61] behaves differently from the dynamics of systems we have previously studied, including aromatic disulfide exchange (representing a [2 + 1] radical-mediated exchange with aspects of both associative and dissociative chemistry[56–58]) and dialkylamine disulfide exchange (a fully dissociative chemistry[51–54]). In particular, both of the aforementioned disulfide dynamic chemistries involve the production of sulfur radicals while the chemistry is active.[51,57] Although that did not hinder the synthesis and reprocessability of CANs made by reactive processing using these chemistries,[38,39,42,44] it was unknown how the use of a dynamic chemistry that did not rely on radical reactions when active would impact the production and performance of polyolefin CANs.

Using the r-EOC precursor, we conducted loading tests to identify a formulation that would yield robust, reprocessable CANs and could then be applied to our other polyolefin precursors. We did so by synthesizing a range of reactively processed materials using either a constant wt% of BBMA and a varied wt% of DCP (Fig. 1a) or a varied wt% of BBMA and a constant wt% of DCP (Fig. 1b). We used tension-mode, small-amplitude oscillatory dynamic mechanical analysis (DMA) to assess the robustness of each sample by measuring the tensile storage modulus (E') as a function of temperature. Subsequently, the sample was evaluated for reprocessability by cutting it up and remolding it under the same conditions that produced the 1st mold (160 °C for 1.0 h), and a sample was considered reprocessable if the 2nd mold was fully healed (Fig. S1).

By first examining the samples with various DCP loadings (Fig. 1a), we found that materials containing 0.75 and 1 wt% DCP exhibited robust plateaus in E' but could not be reprocessed into fully healed films, indicating excessive permanent cross-links; in contrast, materials with 0.5 and 0.6 wt% DCP fully healed upon reprocessing, confirming their character as CANs. The CAN with 0.6 wt% DCP yielded the higher E' values of the two while still retaining reprocessability (Fig. S1); thus, we used this DCP loading as the standard for testing variations in BBMA loading (Fig. 1b). Each of the three materials tested (containing 3, 5, or 7 wt% BBMA) could be reprocessed into healed 2nd-mold films, confirming their status as CANs. We subsequently conducted DMA tests on the 2nd-molded CANs

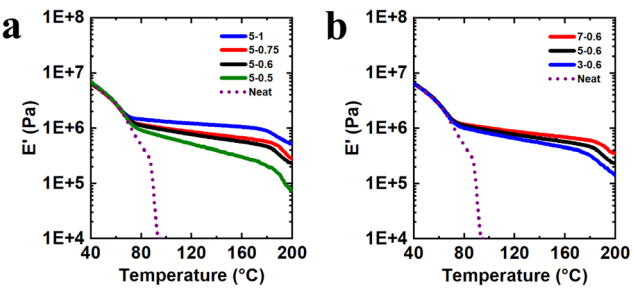

Fig. 1 Tensile storage modulus (E') of cross-linked r-EOC films synthesized with BBMA cross-linker and DCP radical initiator as functions of temperature and loadings of (a) DCP (wt%) or (b) BBMA (wt%). The legends correspond to "wt% of BBMA"–"wt% of DCP"; the tensile storage modulus of a neat r-EOC film is included for comparison. The 5-1 and 5-0.75 compositions are permanently cross-linked.

Open Access Article. Published on 01 mayo 2026. Downloaded on 26/5/2026 06:12:29.
This article is licensed under a Creative Commons Attribution 3.0 Unported Licence.

(Fig. S2) to determine whether each material fully recovered its equilibrium properties, as indicated by replication of the rubbery plateau in E' across the measured temperature range.[74] While the 3 wt% case did not fully recover the plateau values, both the 5 wt% and 7 wt% cases recovered these values within experimental uncertainty across the tested temperature range. Given that our previous studies used a 5 wt% cross-linker loading as the approximately optimal condition for producing reactively processed CANs,[38,39,42,44] we selected 5 wt% BBMA as our standard here to enable the most direct comparisons of material properties. (We also note that the previous studies used 1 wt% DCP,[38,39,42,44] which, in our case, led to excessive permanent cross-linking; we therefore used 0.6 wt% DCP as our standard here for the initiator.) This was largely not a detriment to the robustness of the CANs produced for this study (*vide infra*). As such, we selected 5 wt% BBMA and 0.6 wt% DCP as our standard formulation for CAN production, denoted "5-0.6" in the CAN naming scheme (*e.g.*, 5-0.6 r-EOC CAN).

Before moving to the synthesis of CANs from additional precursors, we examined the evolution of the E' plateau shape at temperatures $\gtrsim$175 °C (Fig. S2). We conducted additional remolding tests on the 5-0.6 r-EOC CAN, yielding 3rd- and 4th-molded materials. We found that each molding step (while fully recovering equilibrium values up to 170 °C) further reduced E' values at ~175 °C and above (Fig. S3 and Table S2). This indicates that the azine chemistry of BBMA is better suited to moderate-temperature applications than the aromatic disulfide chemistry used in our previous reactive processing study with BiPheS methacrylate (BPMA).[44] This result is not unexpected given the significant difference in required reprocessing temperature between our studies on *n*-hexyl methacrylate (HMA) copolymer CANs made with either BPMA or BBMA (reprocessing at 200 °C for BPMA[58] *versus* 120 °C for BBMA[60]), as well as the difference in the compounds' degradation temperature (273 °C for BPMA[58] *versus* 219 °C for BBMA[60]). Still, it is an important consideration for applications such as industrial polymer processing.

Additionally, we examined the possibility of side reactions during the reactive processing procedure by conducting control reactions in solvent between DCP and BBMA (to assess potential homopolymerization) or between DCP and the precursor to BBMA (to assess the potential susceptibility of the azine moiety to radical reactions). As shown in Fig. S4a, homopolymerization occurred in the BBMA/DCP mixture at a 5-0.6 ratio; similarly, as shown qualitatively in Fig. S4b and quantitatively in Fig. S4c, product evolution was observed in the precursor/DCP mixture at the same ratio. However, we note that our control reaction conditions represented an extreme case relative to our reactive processing conditions (reactions were conducted at 140 °C for 12 h, as using our reactive processing temperature of 160 °C would cause solvent boiling issues),[47] with reactions occurring on a much longer time scale and in the absence of precursor polymer (which, when present, provides many sites for radical reactions and thus cross-linker grafting rather than side reactions). Given the demonstrated efficacy of our reactive processing procedure in producing reprocessable r-EOC CANs from BBMA and DCP, although side reactions may occur, their presence is not at a level significant enough to detract from the successful incorporation of dynamic BBMA cross-links.

Finally, although the 5-0.6 composition is our standard for this study, variations in properties among our precursor materials suggest that additional formulations may improve performance. For instance, increasing the DCP loading to 1 wt% when synthesizing a CAN from the LDPE precursor yields a higher E' plateau modulus (0.21 MPa at 160 °C, compared to 0.11 MPa for the 5-0.6 formulation) while retaining full reprocessability across multiple molds (Fig. S5). For consistency across the range of precursor polyolefins, all subsequent CANs were prepared using 5 wt% BBMA and 0.6 wt% DCP unless noted otherwise.

3.2. Synthesis and characterization of reactively processed BBMA-based CANs

With our standard values for cross-linker and initiator loadings determined, we synthesized CANs from our precursor polyolefins using the 5-0.6 formulation. We first characterized the resulting materials by DSC, TGA, and gel content measurements (Table 2). As observed in prior reactive processing studies,[38,39,42,44] the cross-linking procedure reduces crystallinity and melting transition values for each CAN relative to its neat precursor, as cross-links disrupt the formation of crystal lamellae. TGA measurements indicated that the operational window for the CANs extended well above the established processing temperature of 160 °C, with T_d values of 337 °C or higher. Each CAN also exhibited a gel content exceeding 50%, confirming network formation, with gel contents largely overlapping within experimental uncertainty. These results were reasonably consistent with those of our previous BPMA reactive processing study,[44] with the LLDPE CAN again exhibiting the highest gel content (outside the range of experimental uncertainty of all but the OBC CAN). The general overlap in gel content values again indicates a lack of a strong relationship between gel content and cross-link density (measured by DMA, *vide infra*), as we have previously noted.[39,42,44]

Each 1st-molded 5-0.6 CAN underwent DMA testing to verify the formation of a robust network, as indicated by a rubbery plateau in E'. In contrast to their neat counterparts, which melted and flowed at elevated temperatures due to the lack of a network structure, each of the PE CANs (Fig. 2 and Table 3) and the copolymer CANs (Fig. 3 and Table 4) exhibited robust rubbery plateaus beginning just above $T_{m,endpoint}$ and decreasing slightly in magnitude with increasing temperature. Reprocessing of CANs into 2nd and 3rd molds (each step involving 1.0 h of compression molding at 160 °C, with an example shown in Fig. S1) and testing the subsequent molds by DMA indicated full recovery within experimental uncertainty of plateau modulus values (Tables 3 and 4). From ideal rubber elasticity theory,[74] we know that

$$E = 3\nu RT \quad (1)$$

This journal is © The Royal Society of Chemistry 2026

Open Access Article. Published on 01 mayo 2026. Downloaded on 26/5/2026 06:12:29.
This article is licensed under a Creative Commons Attribution 3.0 Unported Licence.

Table 2 Properties of 1st-molded CANs

Material	Crystallinity[a] (%)	$T_{m,peak}$ [a] (°C)	$T_{m,endpoint}$ [a] (°C)	T_d [b] (°C)	Gel content[c] (%)
5-0.6 LDPE CAN	39	110	113	374	56 ± 6
5-0.6 LLDPE CAN	42	120	123	346	75 ± 3
5-0.6 HDPE CAN	59	130	134	337	63 ± 3
5-0.6 r-EOC CAN	16	62	74	339	63 ± 5
5-0.6 OBC CAN	14	119	123	337	70 ± 5

[a] Determined by DSC. Listed values are ±1% or 1 °C. [b] Determined by TGA. [c] Determined by swelling in *o*-xylene at 120 °C for 18 h. Error bars represent one standard deviation of three measurements.

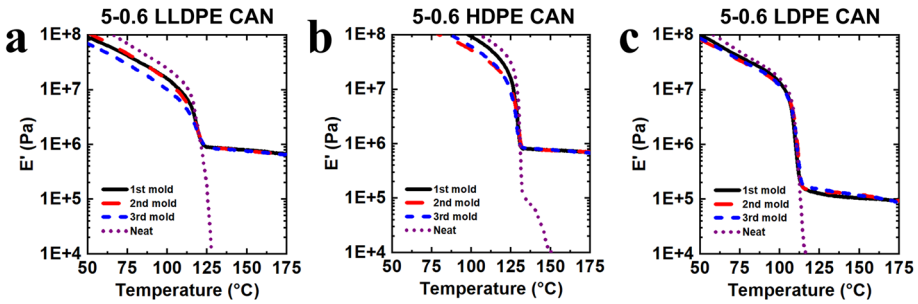

Fig. 2 Tensile storage modulus (E') as a function of temperature and molding step for (a) LLDPE CAN, (b) HDPE CAN, and (c) LDPE CAN, all containing 5 wt% BBMA and 0.6 wt% DCP. Neat counterparts are included for comparison.

Table 3 Tensile storage modulus (E') as a function of molding step and temperature for PE-based samples

		E'[a] (MPa)				
Sample	Mold	130 °C	140 °C	150 °C	160 °C	170 °C
Neat LLDPE	—	0.004	0.002	0.002	0.002	—
5-0.6 LLDPE CAN	1st	0.91 ± 0.03	0.86 ± 0.02	0.82 ± 0.03	0.78 ± 0.03	0.73 ± 0.03
	2nd	0.91 ± 0.03	0.86 ± 0.04	0.82 ± 0.04	0.78 ± 0.05	0.72 ± 0.05
	3rd	0.90 ± 0.12	0.86 ± 0.12	0.81 ± 0.13	0.76 ± 0.12	0.72 ± 0.15
Neat HDPE	—	1.61	0.061	0.011	0.006	0.004
5-0.6 HDPE CAN	1st	1.08 ± 0.09	0.76 ± 0.07	0.74 ± 0.07	0.71 ± 0.06	0.69 ± 0.07
	2nd	1.12 ± 0.12	0.73 ± 0.05	0.70 ± 0.05	0.68 ± 0.05	0.66 ± 0.06
	3rd	1.11 ± 0.11	0.73 ± 0.08	0.70 ± 0.07	0.67 ± 0.08	0.62 ± 0.09
Neat LDPE	—	0.003	0.002	0.001	0.001	—
5-0.6 LDPE CAN	1st	0.12 ± 0.01	0.11 ± 0.01	0.10 ± 0.02	0.09 ± 0.02	0.09 ± 0.02
	2nd	0.15 ± 0.02	0.13 ± 0.02	0.12 ± 0.01	0.11 ± 0.01	0.10 ± 0.01
	3rd	0.16 ± 0.03	0.14 ± 0.03	0.13 ± 0.03	0.12 ± 0.03	0.11 ± 0.03

[a] Determined by DMA. Error bars represent one standard deviation of three measurements.

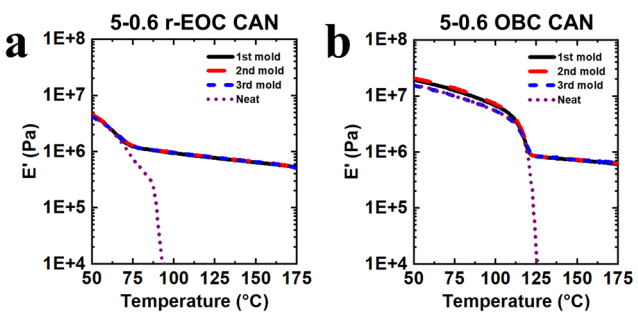

Fig. 3 Tensile storage modulus (E') as a function of temperature and molding step for (a) r-EOC CAN and (b) OBC CAN, made with 5 wt% BBMA and 0.6 wt% DCP. Neat copolymers are included as controls.

where E is the rubbery-plateau tensile modulus, ν is the cross-link density, T is the absolute temperature, and R is the gas constant. By using E' in the rubbery plateau to approximate E, the replication of E' values within experimental uncertainty from mold to mold indicates the full recovery of cross-link density for each CAN after multiple reprocessing cycles and thus the versatility of the BBMA chemistry in imparting dynamic network character to a range of precursor polymers.

We note that the decrease in the rubbery plateau E' with increasing temperature for each polyolefin CAN contrasts with our previous study of HMA–BBMA copolymer CANs,[60] in which the copolymer CAN exhibited an increase in rubbery plateau E' directly proportional to absolute temperature. Per eqn (1), this

Open Access Article. Published on 01 mayo 2026. Downloaded on 26/5/2026 06:12:29.
This article is licensed under a Creative Commons Attribution 3.0 Unported Licence.

Table 4 Tensile storage modulus (E') as a function of molding step and temperature for r-EOC- and OBC-based samples

Sample	Mold	E'^{a} (MPa)				
		130 °C	140 °C	150 °C	160 °C	170 °C
Neat r-EOC	—	0.002	0.002	0.001	0.001	—
5-0.6 r-EOC CAN	1st	0.73 ± 0.02	0.68 ± 0.02	0.63 ± 0.01	0.58 ± 0.02	0.54 ± 0.02
	2nd	0.73 ± 0.04	0.68 ± 0.04	0.64 ± 0.03	0.59 ± 0.02	0.55 ± 0.02
	3rd	0.75 ± 0.01	0.70 ± 0.01	0.64 ± 0.01	0.60 ± 0.01	0.54 ± 0.03
Neat OBC	—	0.004	0.002	0.002	0.001	—
5-0.6 OBC CAN	1st	0.84 ± 0.08	0.80 ± 0.07	0.75 ± 0.08	0.71 ± 0.07	0.66 ± 0.07
	2nd	0.84 ± 0.02	0.79 ± 0.03	0.76 ± 0.02	0.72 ± 0.03	0.68 ± 0.04
	3rd	0.86 ± 0.10	0.80 ± 0.11	0.77 ± 0.10	0.73 ± 0.11	0.68 ± 0.10

[a] Determined by DMA. Error bars represent one standard deviation of three measurements.

indicated that a constant cross-link density was maintained across the rubbery plateau,[74] consistent with BBMA's azine dynamic chemistry being associative in nature.[60,61] Despite the associative nature of BBMA cross-links, our polyolefin CANs do not exhibit a constant cross-link density; however, this result is not unprecedented. Our previous studies on BPMA-based HMA copolymer CANs[58] and reactively processed polyolefin CANs[44] similarly indicated that the copolymer CANs behaved in an ideal associative manner (maintaining a constant cross-link density in the rubbery plateau). In contrast, the polyolefin CANs exhibited a reduction in cross-link density with increasing temperature, a result independent of applied frequency.[44] (We confirmed this frequency-independent behavior in our BBMA-based polyolefin CANs under the same testing conditions; see Fig. S6.) Given similar findings in a study by Du Prez and coworkers,[75] as well as other studies from our group indicating distinctions in material behavior resulting from differing methods of cross-linker incorporation,[38,46,54] deeper future examinations are warranted on the temperature-dependent dynamics of reactively processed CANs containing associative cross-links.

By examining the plateau modulus at a specific temperature, we can compare the cross-link densities of our polyolefin CANs. Using 160 °C as our standard, we found that the rubbery plateau E' values (and thus cross-link densities) follow this trend: 5-0.6 LLDPE CAN ~ 5-0.6 HDPE CAN ~ 5-0.6 OBC CAN > 5-0.6 r-EOC CAN > 5-0.6 LDPE CAN. Our prior study on BPMA-based polyolefin CANs[44] exhibited almost the same trend, except that the BPMA-based LLDPE CAN exhibited a higher E' than the HDPE and OBC CANs (rather than all three being approximately on par as we see in this study). However, comparing the E' values at 160 °C between our BBMA-based CANs and our previous BPMA-based CANs reveals an important difference: except for the LDPE case, the BBMA-based CANs exhibit E' values comparable to or up to ~50% higher than BPMA-based CANs, despite using less DCP (0.6 wt% *vs.* 1.0 wt%). According to eqn (1), this means that a 40% reduction in radical initiator still enables our BBMA-based CANs to incorporate up to 50% more cross-links than our previous BPMA-based CANs. (Increasing the DCP loading to 1.0 wt% for the BBMA-based LDPE CAN, matching the loading in our BPMA reactive processing study,[44] results in an E' value at 160 °C that slightly exceeds that of the BPMA-based version; see Fig. S5.) The greater effectiveness of BBMA in introducing cross-links is supported by our earlier study on an HMA–BBMA copolymer CAN,[60] which found that the cross-link density maintained across the rubbery plateau was 36% higher than that of an HMA–BPMA copolymer CAN[58] synthesized with the same molar amount of cross-linker. Thus, whether through free-radical copolymerization or radical-based reactive processing, BBMA enables higher cross-link densities than BPMA at equivalent loadings. Furthermore, our prior work shows BPMA can produce more cross-links in polyolefin CANs than BiTEMPS methacrylate (BTMA) at the same loading;[38,44] this indicates that BBMA is also more effective than BTMA for cross-linking polyolefins, making BBMA the most efficient cross-linker for producing polyolefin CANs we have studied to date.

3.3. Creep testing and alternative processing methods for reactively processed BBMA-based CANs

Given the importance of suppressing elevated-temperature creep in polyolefin networks for potential high-temperature applications, we sought to confirm that our previous findings on the substantial creep resistance of an HMA–BBMA copolymer[60] remained applicable to our BBMA-based polyolefin CANs. Accordingly, we conducted creep tests on the CANs at 150 °C under a shear stress of 3.0 kPa for 10 000 s to assess their creep resistance in the molten state (Fig. 4a–c and Table S3). When compared to their neat precursors (insets of Fig. 4a–c), which exhibited substantial creep over a much shorter time frame of 200 s (Table S4), each of the CANs showed creep suppressed by multiple orders of magnitude due to the incorporated BBMA cross-links. Indeed, calculation of the viscous creep strains of the CANs (obtained by extrapolating the linear fit of the creep data between t = 9000 s and t = 10 000 s back to t = 0 s and subtracting the y-intercept from the total strain at t = 10 000 s) indicated that the greatest amount of viscous creep strain, exhibited by the 5-0.6 LDPE CAN, was 19%, an outstanding reduction when compared to the 9000% strain experienced by the neat LDPE over a much shorter 200 s time frame. Given that these measurements were taken only 10 °C below the reprocessing temperature of the

This journal is © The Royal Society of Chemistry 2026

Open Access Article. Published on 01 mayo 2026. Downloaded on 26/5/2026 06:12:29.
This article is licensed under a Creative Commons Attribution 3.0 Unported Licence.

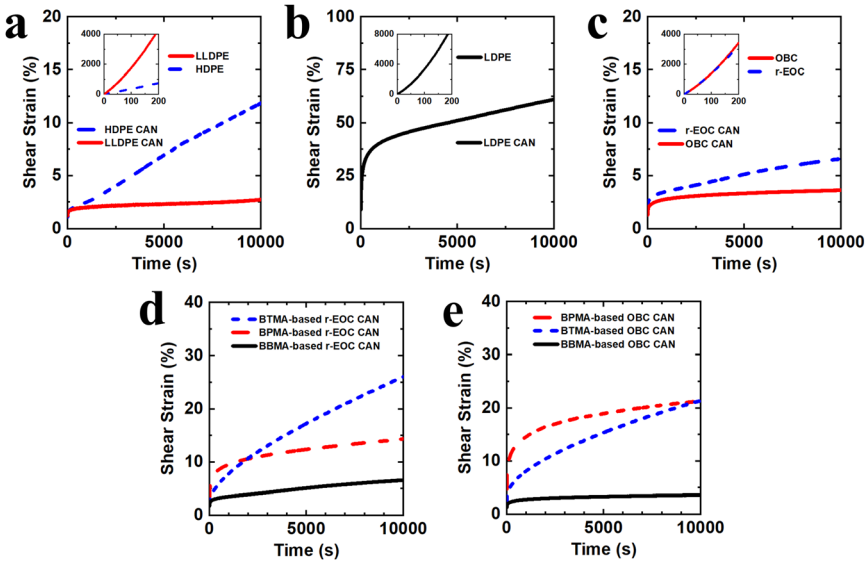

Fig. 4 (a)/(b)/(c) Elevated-temperature creep response: shear strain (%) as a function of time for neat precursors (insets) and CANs made with (a) LLDPE or HDPE, (b) LDPE, or (c) r-EOC or OBC. Each sample was subjected to a 3.0 kPa shear load at 150 °C for 10 000 s. All CANs contain 5 wt% BBMA and 0.6 wt% DCP. (d)/(e) Comparison of elevated-temperature creep behavior of CANs containing 5 wt% of BBMA, BPMA (BiPheS methacrylate), or BTMA (BiTEMPS methacrylate) and made from (d) r-EOC or (e) OBC. The BBMA-based CAN contains 0.6 wt% DCP while the BPMA- and BTMA-based CANs contain 1 wt% DCP. Each sample was subjected to a 3.0 kPa shear load at 150 °C for 10 000 s. The BPMA- and BTMA-based data were adapted with permission from ref. 44.

CANs, these findings indicate that the associative nature of BBMA's azine dynamic chemistry enables facile reprocessability at pressure and/or shear-rate conditions associated with elevated-temperature compression molding, extrusion, *etc.*, while still maintaining a robust network structure at conditions associated with (near) atmospheric pressure and (near) zero-shear-rate conditions.

Use of the 150 °C testing temperature also enabled direct comparisons with creep tests performed on BPMA- and BTMA-based polyolefin CANs in our previous study (Fig. 4d, e and Table S5).[44] We previously demonstrated that replacing BTMA with BPMA reduced viscous creep by 77% and 60% in r-EOC and OBC CANs, respectively, when incorporated using the same formulation on a mass basis (5 wt% cross-linker, 1 wt% DCP).[44] Here, we found that BBMA provided even greater reductions in creep; relative to BPMA, BBMA reduced creep by 41% in the r-EOC case (Fig. 4d) and by 86% in the OBC case (Fig. 4e) while using less DCP (0.6 wt% *vs.* 1.0 wt%). This comparison further supports our assertion that BBMA is more effective at introducing cross-links than BPMA, as the ~50% higher cross-link density exhibited by the 5-0.6 r-EOC and OBC CANs (compared to their 5-1 BPMA-based counterparts) provided greater resistance to creep, as would be expected from a more highly cross-linked system.

Analyzing the creep responses in the BBMA-based and BPMA-based PE CANs revealed a complex picture. In the LLDPE case, the 5-0.6 BBMA-based CAN had a cross-link density comparable to that of the 5-1 BPMA-based CAN,[44] yet it showed an 86% reduction in viscous creep. For HDPE, both the 5-0.6 BBMA-based CAN and the 5-1 BPMA-based CAN[44] exhibited similar cross-link densities and viscous creep strains. These results indicate that, at the same cross-link levels, BBMA provides equal or superior resistance to viscous creep compared to BPMA. Because the BBMA dynamic chemistry is fully associative when active,[60,61] whereas the BPMA dynamic chemistry is primarily associative but involves a dissociative component,[56–58] it is reasonable that a system with a small proportion of dissociated cross-links would exhibit more viscous creep than a fully associative system. However, in the LDPE case, the 5-0.6 BBMA-based CAN exhibited greater viscous creep than the 5-1 BPMA-based CAN,[44] albeit while having a lower cross-link density. This was confirmed by synthesizing a 5-1 BBMA-based CAN, which had a cross-link density similar to the 5-1 BPMA case but exhibited a higher viscous creep strain (although, as expected, the viscous creep strain was lower than the 5-0.6 BBMA case; see Fig. S7 and Table S3). Interestingly, the 5-1 BPMA-based LDPE CAN from our earlier study exhibited the lowest viscous creep strain among the tested polyolefin CANs despite also having the lowest cross-link density,[44] suggesting this result may be an outlier. Future studies are warranted to investigate how precursor polyolefin microstructure and properties, as well as the choice of the dynamic cross-linker, affect the viscous creep behavior of the resulting reactively processed polyolefin CANs.

We also used the long-time linear fits of the creep curves to calculate the zero-shear-rate viscosity (at 150 °C) of each BBMA-based polyolefin CAN (Table S3), using the viscous dashpot element of the Burgers model in our analysis:[76]

$$\eta_0 = \tau_0/\dot{\gamma} \quad (2)$$

Open Access Article. Published on 01 mayo 2026. Downloaded on 26/5/2026 06:12:29.
This article is licensed under a Creative Commons Attribution 3.0 Unported Licence.

where η_0 is the zero-shear-rate viscosity, τ_0 is the applied shear stress, and $\dot{\gamma}$ is the steady-state creep strain rate. In doing so, we sought to compare our results with our previous HMA-BBMA copolymer system,[60] which exhibited very high creep (effectively zero-shear-rate) viscosities and thus very low viscous creep across a wide temperature range. This lack of melt flow exhibited by the copolymer under testing conditions (notably, near-ambient pressure) seemed to preclude reprocessing; nevertheless, the copolymer was successfully reprocessed into healed material *via* compression molding and injection molding (albeit with a reduced plateau modulus in the latter case and limited success when attempting extrusion).[60] As such, our previous work indicated the necessity of elevated pressure (resulting from processing procedures such as compression molding) in inducing melt flow and thus enabling reprocessing when BBMA is employed in a copolymer CAN system;[60] therefore, we sought to determine whether similar results would be observed for our reactively processed CANs. By comparing the zero-shear-rate viscosities obtained from the creep tests in both studies, we found that while the HMA–BBMA copolymer maintained a viscosity on the order of 10^{11} Pa s from 120–190 °C,[60] the highest viscosity exhibited by our polyolefin CANs at 150 °C was the 5-0.6 OBC case, with a value of 5.3×10^9 Pa s. Given the significant reduction in viscosity when BBMA was incorporated *via* reactive processing, as well as our continued success in reprocessing our CANs *via* compression molding, we anticipated greater success in property recovery with the alternative, industrially relevant, high-shear-rate processing methods than we saw for our copolymer case.

We therefore conducted injection molding and extrusion tests on our 5-0.6 r-EOC CAN at 160 °C to compare directly with our previous compression molding results at the same temperature. We synthesized 1st-molded films of our CAN *via* compression molding (Fig. 5a), cut them into pieces, and fed them into a HAAKE MiniLab 3 extruder, cycling the material through the machine for 5 min at 160 °C. At this point, we either removed the CAN from the cycling chamber, yielding a sample representative of injection molding (Fig. 5b), or extruded the material through the outlet (Fig. 5c). It was immediately evident that our r-EOC CAN was easier to extrude than our previous copolymer CAN,[60] as the material fully fused upon exiting the outlet (Fig. S8), unlike the crumbly, partial fusion seen before. DMA measurements (Fig. 5d) corroborated this, showing the extrudate maintained a quasi-rubbery plateau in E' throughout the temperature ramp. The injection-molded sample behaved similarly, which stood in contrast to the injection-molded copolymer CAN of our previous study (which fractured at ~150 °C).[60] However, a key similarity in rubbery plateau values was observed: the injection molded sample exhibited a reduction in E' relative to the compression molded sample, and the extruded sample's E' plateau was yet further reduced. This suggests that the necessity of elevated pressure for successful BBMA reprocessing remains valid for reactively processed CANs, as the higher pressure inside the cycling chamber results in a greater recovery of plateau modulus than the reduction to ambient pressure experienced when extruding the CAN from the machine's outlet. Thus, although a precursor polyolefin may enable extrudability, the high pressure needed for BBMA exchange continues to limit the full reprocessability/property recovery. Based on this and our earlier finding on the more moderate-temperature suitability of BBMA relative to BPMA,[44,58,60] future study should focus on optimizing the processing conditions to fully recover equilibrium properties when reprocessing BBMA CANs using methods like injection molding or extrusion.

Finally, to provide another point of comparison with our previous copolymer CAN,[60] we conducted stress relaxation measurements on the 5-0.6 CANs made using LDPE, r-EOC, and OBC (representing the CANs that underwent the highest, median, and lowest viscous creep strains, respectively, as indicated in Table S3) from 140–170 °C, resulting in the normalized profiles seen in Fig. S9. We then fit these profiles to a

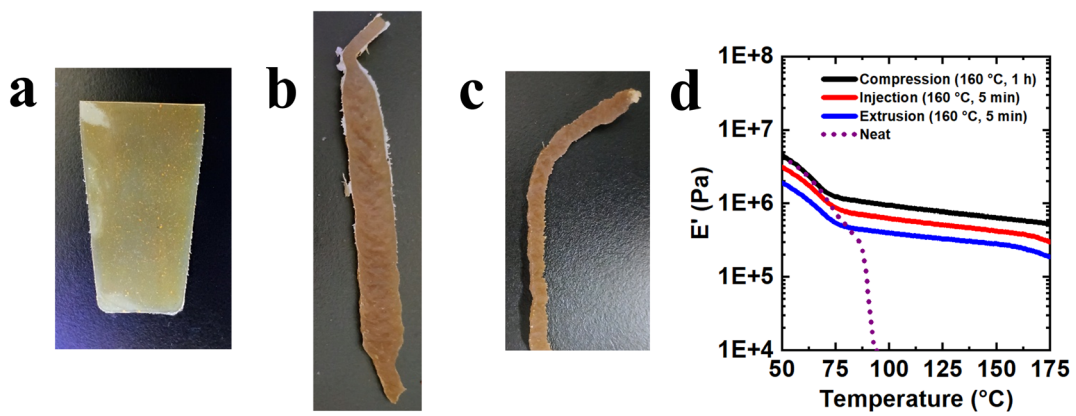

Fig. 5 5-0.6 r-EOC CANs: (a) sample produced after 1.0 h of compression molding at 160 °C, and (b)/(c) samples produced after 5 min of residence time in the extruder, representing (b) injection molding at 160 °C and (c) extrusion at 160 °C. (d) Tensile storage modulus (E') of the 5-0.6 r-EOC CAN samples as functions of temperature and processing conditions (temperatures and times in the legend represent the conditions used for each processing procedure). The E' values at 160 °C are 0.60, 0.39, and 0.26 MPa for the compression-molded, injection-molded, and extruded samples, respectively.

This journal is © The Royal Society of Chemistry 2026

Open Access Article. Published on 01 mayo 2026. Downloaded on 26/5/2026 06:12:29.
This article is licensed under a Creative Commons Attribution 3.0 Unported Licence.

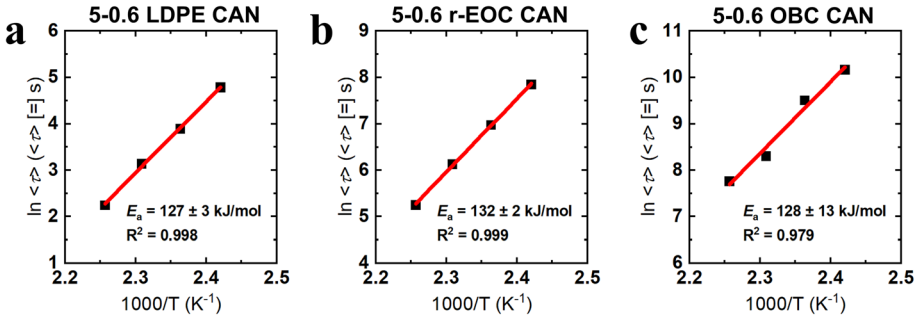

Fig. 6 Arrhenius plots showing the apparent activation energy (E_a) of stress relaxation in the 5-0.6 CANs made from (a) LDPE, (b) r-EOC, and (c) OBC.

stretched exponential decay function to account for the breadth of relaxation times typically observed in polymers and dynamic networks:[77,78]

$$\frac{E(t)}{E_0} = \exp\left[-\left(\frac{t}{\tau^*}\right)^{\beta}\right] \quad (3)$$

This enabled us to extract a characteristic relaxation time, τ^*, and a stretching exponent, β, for each CAN at each tested temperature, which then allowed us to calculate $\langle\tau\rangle$, the average relaxation time:[79]

$$\langle\tau\rangle = \frac{\tau^* \Gamma(1/\beta)}{\beta} \quad (4)$$

where Γ is the gamma function. Both the fitting parameters and the $\langle\tau\rangle$ values for each CAN at each temperature are listed in Table S6. In contrast to the copolymer CAN, which exhibited extremely slow stress relaxation at temperatures as high as 210 °C (preventing fitting by the aforementioned methods),[60] the polyolefin CANs exhibited more rapid relaxation, with resulting relaxation times consistent with the existing trends of the materials in viscous creep strain (more viscous creep corresponds to a shorter average relaxation time) and cross-link density (higher cross-link density corresponds to a longer average relaxation time).

We constructed Arrhenius plots from the $\langle\tau\rangle$ values for each CAN at the tested temperatures to determine the activation energy for stress relaxation in each case (Fig. 6). Over the 140–170 °C temperature range, each CAN exhibits, within experimental uncertainty, the same activation energy of ~130 kJ mol^{-1}. This indicates a fundamental similarity in the relaxation mechanism of these CANs which holds true regardless of the variations in the magnitude of the $\langle\tau\rangle$ values for each of the individual CAN cases. Given our previous studies on the viscoelastic behavior of CANs containing associative cross-links,[58,80] and our previous demonstration of BBMA's associative character in HMA–BBMA copolymer CANs,[60] we might expect the activation energy to align with the alpha-relaxation of the precursor polymers. However, those values fall within the range of 60–100 kJ mol^{-1}.[42] If we instead consider CANs containing dissociative cross-links, which is consistent with the observed decrease in storage modulus with increasing temperature in the quasi-rubbery plateau (see Fig. 2, 3, and 5), we might expect the activation energy to align with the bond dissociation energy of the azine bond at the center of BBMA, which is ~200–250 kJ mol^{-1}.[81] Given that the activation energy value we obtain is distinct from both of these cases, future study is warranted to explore the fundamental underpinnings of the stress relaxation dynamics in polyolefin CANs made with BBMA dynamic covalent cross-linkers.

4. Conclusions

We utilized radical-based reactive processing to incorporate azine dynamic covalent cross-links into polyolefin precursor materials. Using an azine-based methacrylate cross-linker, BBMA, and a radical initiator, DCP, we grafted associative dynamic cross-links (which undergo [2 + 2] metathesis when active[60,61]) between the chains of the precursor materials, producing CANs made from PE and ethylene-containing copolymers. Initial formulation tests led us to select a standard composition of 5 wt% BBMA and 0.6 wt% DCP to create robust, reprocessable CANs, evidenced by the complete recovery of E' rubbery plateau modulus values after remolding. CANs made from our range of precursor materials using this composition showed significant network formation, confirmed by gel content and DMA measurements, and maintained the equilibrium plateau modulus across three molding cycles, demonstrating the preservation of CAN cross-link density upon reprocessing.[74] Compared to our previous study using aromatic-disulfide-based BPMA cross-links to synthesize polyolefin CANs,[44] we observed that the use of BBMA at the same loading produced E' plateau modulus values on par with or up to 50% greater than those of the previous CANs while using less DCP (0.6 wt% *vs.* 1.0 wt%). This finding underscores BBMA's superior effectiveness in introducing dynamic cross-links within CANs (as supported by previous HMA–BBMA and HMA–BPMA copolymerization studies[58,60]).

Elevated-temperature, long-time creep tests showed that our BBMA-based CANs exhibited substantial creep suppression compared with their neat counterparts, which experienced

Open Access Article. Published on 01 mayo 2026. Downloaded on 26/5/2026 06:12:29.
This article is licensed under a Creative Commons Attribution 3.0 Unported Licence.

orders-of-magnitude higher creep over a much shorter time scale. Additionally, our BBMA-based CANs generally exhibited creep resistance equal to or better than that of BPMA-based CANs[44] while using less radical initiator. This trend also applied to CANs with dialkylamine-disulfide-based BTMA cross-links.[44] Besides their notable elevated-temperature creep resistance, our BBMA-based polyolefin CANs exhibited lower zero-shear-rate viscosities than those obtained from HMA–BBMA copolymer CANs,[60] indicating a greater suitability for reprocessing *via* injection molding and extrusion, methods that had encountered some difficulties with the copolymer CANs. We successfully produced healed materials using these industrially relevant processing methods. Although our findings confirmed that the exchange of the BBMA chemistry remains pressure-dependent, these methods are applicable for reprocessing BBMA-based polyolefin CANs. Overall, our BBMA-based CANs match or exceed the E' plateau modulus values and creep resistance of previous BTMA-based and BPMA-based CANs,[44] require less radical initiator, allow milder reprocessing temperatures, and are amenable to a variety of processing methods.

Conflicts of interest

A US patent application has been filed that is related to the research described in this manuscript.

Data availability

The data supporting this article are included as part of the supplementary information (SI). Supplementary information: molecular weight data for neat precursor polymers, image of successful reprocessing, additional DMA temperature ramps and frequency sweeps for various CANs, additional storage modulus data for the 5-0.6 r-EOC CAN, side-reaction control experiments, viscous creep strains and additional creep-derived data for various CANs, additional creep plot for the 5-1 LDPE CAN, image of extrudate, stress relaxation plots and quantitative data for various CANs. See DOI: https://doi.org/10.1039/d6py00172f.

Acknowledgements

This research was supported by the University Partnership Initiative between Northwestern University and The Dow Chemical Company. We also acknowledge support from Northwestern University *via* discretionary funds associated with a Walter P. Murphy Professorship. This work made use of the MatCI/CLAMMP/MLTOF Facility at Northwestern University, which receives support from the MRSEC Program (NSF DMR-2308691) of the Materials Research Center at Northwestern University. We thank Subeen Kim for assistance with extrusion testing.

References

1 D. Jeremic, in *Ullmann's Encyclopedia of Industrial Chemistry*, John Wiley & Sons, Ltd, 2014, pp. 1–42.
2 R. Geyer, J. R. Jambeck and K. L. Law, *Sci. Adv.*, 2017, **3**, e1700782.
3 X.-Y. Wang, Y. Gao and Y. Tang, *Prog. Polym. Sci.*, 2023, **143**, 101713.
4 W. Kaminsky and H. Sinn, *Transition Metals and Organometallics as Catalysts for Olefin Polymerization*, Springer-Verlag, 1988.
5 R. Quijada, J. Dupont, M. S. L. Miranda, R. B. Scipioni and G. B. Galland, *Macromol. Chem. Phys.*, 1995, **196**, 3991–4000.
6 D. J. Arriola, E. M. Carnahan, P. D. Hustad, R. L. Kuhlman and T. T. Wenzel, *Science*, 2006, **312**, 714–719.
7 H. P. Wang, S. P. Chum, A. Hiltner and E. Baer, *J. Appl. Polym. Sci.*, 2009, **113**, 3236–3244.
8 OECD, *Global Plastics Outlook: Economic Drivers, Environmental Impacts and Policy Options*, OECD Publishing, 2022.
9 M. Lazár, R. Rado and J. Rychlý, in *Polymer Physics*, Springer, Berlin, Heidelberg, 1990, pp. 149–197.
10 R. Patterson, A. Kandelbauer, U. Müller and H. Lammer, in *Handbook of Thermoset Plastics*, ed. H. Dodiuk, Elsevier, Amsterdam, 3rd edn, 2014, pp. 697–737.
11 M. Selvin, S. Shah, H. J. Maria, S. Thomas, R. Tuladhar and M. Jacob, *Ind. Eng. Chem. Res.*, 2024, **63**, 1200–1214.
12 A. J. Shapiro, P. J. Brigandi, M. Moubarak, S. S. Sengupta and T. H. I. Epps, *ACS Appl. Polym. Mater.*, 2024, **6**, 11859–11876.
13 X. Chen, M. A. Dam, K. Ono, A. Mal, H. Shen, S. R. Nutt, K. Sheran and F. Wudl, *Science*, 2002, **295**, 1698–1702.
14 C. J. Kloxin, T. F. Scott, B. J. Adzima and C. N. Bowman, *Macromolecules*, 2010, **43**, 2643–2653.
15 D. Montarnal, M. Capelot, F. Tournilhac and L. Leibler, *Science*, 2011, **334**, 965–968.
16 M. Capelot, M. M. Unterlass, F. Tournilhac and L. Leibler, *ACS Macro Lett.*, 2012, **1**, 789–792.
17 C. J. Kloxin and C. N. Bowman, *Chem. Soc. Rev.*, 2013, **42**, 7161–7173.
18 W. Zou, J. Dong, Y. Luo, Q. Zhao and T. Xie, *Adv. Mater.*, 2017, **29**, 1606100.
19 L. Li, X. Chen, K. Jin and J. M. Torkelson, *Macromolecules*, 2018, **51**, 5537–5546.
20 L. Li, X. Chen, K. Jin, M. A. Bin Rusayyis and J. M. Torkelson, *Macromolecules*, 2021, **54**, 1452–1464.
21 V. Zhang, B. Kang, J. V. Accardo and J. A. Kalow, *J. Am. Chem. Soc.*, 2022, **144**, 22358–22377.
22 S. Maes, N. Badi, J. M. Winne and F. E. Du Prez, *Nat. Rev. Chem.*, 2025, **9**, 144–158.
23 A. Toldy, D. I. Poór, N. Geier and Á. Pomázi, *Composites, Part B*, 2025, **306**, 112760.
24 X. Chen, L. Li and J. M. Torkelson, *Polymer*, 2019, **178**, 121604.
25 L. Li, X. Chen and J. M. Torkelson, *ACS Appl. Polym. Mater.*, 2020, **2**, 4658–4665.

 This journal is © The Royal Society of Chemistry 2026

Open Access Article. Published on 01 mayo 2026. Downloaded on 26/5/2026 06:12:29.
This article is licensed under a Creative Commons Attribution 3.0 Unported Licence.

26 X. Chen, L. Li, K. Jin and J. M. Torkelson, *Polym. Chem.*, 2017, **8**, 6349–6355.
27 J. P. Brutman, D. J. Fortman, G. X. De Hoe, W. R. Dichtel and M. A. Hillmyer, *J. Phys. Chem. B*, 2019, **123**, 1432–1441.
28 L. Hammer, N. J. Van Zee and R. Nicolaÿ, *Polymers*, 2021, **13**, 396.
29 S. Serna, N. S. Purwanto, L. M. Fenimore and J. M. Torkelson, *Polymer*, 2024, **306**, 127232.
30 M. Röttger, T. Domenech, R. van der Weegen, A. Breuillac, R. Nicolaÿ and L. Leibler, *Science*, 2017, **356**, 62–65.
31 F. Caffy and R. Nicolaÿ, *Polym. Chem.*, 2019, **10**, 3107–3115.
32 R. G. Ricarte, F. Tournilhac and L. Leibler, *Macromolecules*, 2019, **52**, 432–443.
33 G. P. Kar, M. O. Saed and E. M. Terentjev, *J. Mater. Chem. A*, 2020, **8**, 24137–24147.
34 R. G. Ricarte, F. Tournilhac, M. Cloître and L. Leibler, *Macromolecules*, 2020, **53**, 1852–1866.
35 M. Maaz, A. Riba-Bremerch, C. Guibert, N. J. Van Zee and R. Nicolaÿ, *Macromolecules*, 2021, **54**, 2213–2225.
36 S. Wang, S. Ma, J. Qiu, A. Tian, Q. Li, X. Xu, B. Wang, N. Lu, Y. Liu and J. Zhu, *Green Chem.*, 2021, **23**, 2931–2937.
37 M. Ahmadi, A. Hanifpour, S. Ghiassinejad and E. van Ruymbeke, *Chem. Mater.*, 2022, **34**, 10249–10271.
38 L. M. Fenimore, B. Chen and J. M. Torkelson, *J. Mater. Chem. A*, 2022, **10**, 24726–24745.
39 B. Chen, L. M. Fenimore, Y. Chen, S. M. Barbon, H. A. Brown, E. Auyeung, C. L. P. Shan and J. M. Torkelson, *Polym. Chem.*, 2023, **14**, 3621–3637.
40 D. Hassanian-Moghaddam, N. Asghari and M. Ahmadi, *Macromolecules*, 2023, **56**, 5679–5697.
41 B. Chen, T. Debsharma, L. M. Fenimore, T. Wang, Y. Chen, N. S. Purwanto and J. M. Torkelson, *Macromol. Rapid Commun.*, 2024, **45**, 2400460.
42 L. M. Fenimore, B. Chen, Y. Chen, S. M. Barbon, H. A. Brown, E. Auyeung, C. L. P. Shan and J. M. Torkelson, *Eur. Polym. J.*, 2024, **202**, 112661.
43 C. R. López-Barrón, J. Lu, J. A. Throckmorton, H. Passino and M. Gopinadhan, *Macromolecules*, 2024, **57**, 2729–2745.
44 M. J. Suazo, L. M. Fenimore, S. M. Barbon, H. Brown, E. Auyeung, G. Cespedes, C. Li Pi Shan and J. M. Torkelson, *ACS Appl. Polym. Mater.*, 2024, **6**, 14772–14783.
45 B. S. Bohra, D. Kundu, B. SanthiBhushan, I. Dey, S. Mandal and S. Bose, *Chem. Eng. J.*, 2025, **525**, 169664.
46 L. M. Fenimore, M. J. Suazo, S. Mitchell, H. Mohammadi, K. M. McLoughlin, C. Gallaschun, P. Sewruk, M. Busch and J. M. Torkelson, *J. Am. Chem. Soc.*, 2025, **147**, 27179–27185.
47 Y.-W. Huang, M. J. Suazo, S. M. Barbon, H. A. Brown, E. Auyeung, C. Li Pi Shan and J. M. Torkelson, *ACS Macro Lett.*, 2025, **14**, 341–348.
48 Y.-W. Huang, M. J. Suazo and J. M. Torkelson, *Macromolecules*, 2025, **58**, 4847–4859.
49 Y.-W. Huang, M. J. Suazo, S. M. Barbon, H. A. Brown, E. Auyeung, C. Li Pi Shan and J. M. Torkelson, *ChemSusChem*, 2025, **18**, e202501137.
50 W. Soenen, G. Poilvet, A. Sekar, S. Dul, C. Hervieu and S. Gaan, *Sustainable Mater. Technol.*, 2025, **45**, e01638.
51 A. Takahashi, R. Goseki and H. Otsuka, *Angew. Chem., Int. Ed.*, 2017, **56**, 2016–2021.
52 M. A. Bin Rusayyis and J. M. Torkelson, *Macromolecules*, 2020, **53**, 8367–8373.
53 M. A. Bin Rusayyis and J. M. Torkelson, *Polym. Chem.*, 2021, **12**, 2760–2771.
54 T. Debsharma, N. S. Purwanto, L. M. Fenimore, S. Mitchell, J. Kennedy and J. M. Torkelson, *Polym. Chem.*, 2024, **15**, 2167–2176.
55 L. M. Fenimore, M. J. Suazo, B. Chen, S. M. Barbon, H. A. Brown, E. Auyeung, C. Li Pi Shan and J. M. Torkelson, *Macromolecules*, 2025, **58**, 9494–9503.
56 I. Azcune and I. Odriozola, *Eur. Polym. J.*, 2016, **84**, 147–160.
57 J. M. Matxain, J. M. Asua and F. Ruipérez, *Phys. Chem. Chem. Phys.*, 2016, **18**, 1758–1770.
58 M. J. Suazo and J. M. Torkelson, *ACS Appl. Polym. Mater.*, 2024, **6**, 9209–9218.
59 X. Zheng, Z. Liu, L. Yang, K. Li, L. Zhang, Y. Song and Y. Li, *Macromolecules*, 2025, **58**, 4536–4546.
60 M. J. Suazo and J. M. Torkelson, *ACS Macro Lett.*, 2025, **14**, 1248–1255.
61 A.-E. Dascalu, L. Halgreen, A. Torres-Huerta and H. Valkenier, *Chem. Commun.*, 2022, **58**, 11103–11106.
62 X. Xu, S. Ma, S. Wang, J. Wu, Q. Li, N. Lu, Y. Liu, J. Yang, J. Feng and J. Zhu, *J. Mater. Chem. A*, 2020, **8**, 11261–11274.
63 J. Han, Y. Zhou, G. Bai, W. Wei, X. Liu and X. Li, *Mater. Chem. Front.*, 2022, **6**, 503–511.
64 J. Han, M. Dai, G. Bai, M. Wei, J. Liu, W. Wei, X. Liu and X. Li, *Eur. Polym. J.*, 2023, **195**, 112210.
65 J. Han, S. Li, W. Zhang, M. Wei, J. Liu, W. Wei, X. Liu and X. Li, *ACS Appl. Polym. Mater.*, 2024, **6**, 712–721.
66 J. Han, W. Zhang, M. Wei, Y. Zhu, X. Liu and X. Li, *Composites, Part B*, 2024, **284**, 111693.
67 M. Marić and C. W. Macosko, *Polym. Eng. Sci.*, 2001, **41**, 118–130.
68 B. Wunderlich and G. Czornyj, *Macromolecules*, 1977, **10**, 906–913.
69 T. P. Karjala, J. Ortega, L. L. Kardos and J. L. Cooper, *WO Pat*, WO089750A1, 2019.
70 Y.-C. Hsu, R. W. Truss, B. Laycock, M. P. Weir, T. M. Nicholson, C. J. Garvey and P. J. Halley, *Polymer*, 2017, **119**, 66–75.
71 K. L. Nichols, W. J. Michie Jr. and M. Kapur, *US Pat*, US0227144A1, 2010.
72 K. S. Anderson and M. A. Hillmyer, *Polymer*, 2004, **45**, 8809–8823.
73 G. Xu, Y. Xiao, W.-J. Wang, B.-G. Li and P. Liu, *Macromolecules*, 2023, **56**, 3064–3072.
74 P. J. Flory, *Principles of Polymer Chemistry*, Cornell University Press, 1953.
75 C. Taplan, M. Guerre, J. M. Winne and F. E. Du Prez, *Mater. Horiz.*, 2020, **7**, 104–110.

76 W. N. Findley, J. S. Lai and K. Onaran, *Creep and Relaxation of Nonlinear Viscoelastic Materials*, North-Holland Publishing Company, 1976.
77 G. Williams and D. C. Watts, *Trans. Faraday Soc.*, 1970, **66**, 80–85.
78 A. Dhinojwala, J. C. Hooker and J. M. Torkelson, *J. Non-Cryst. Solids*, 1994, **172**, 286–296.
79 J. C. Hooker and J. M. Torkelson, *Macromolecules*, 1995, **28**, 7683–7692.
80 T. Wang, Y. Chen, B. Chen, M. J. Suazo, N. S. Purwanto and J. M. Torkelson, *ACS Macro Lett.*, 2024, **13**, 1147–1155.
81 Y. Zheng, W. Zheng, J. Wang, H. Chang and D. Zhu, *J. Phys. Chem. A*, 2018, **122**, 2764–2780.

Open Access Article. Published on 01 mayo 2026. Downloaded on 26/5/2026 06:12:29.
This article is licensed under a Creative Commons Attribution 3.0 Unported Licence.

This journal is © The Royal Society of Chemistry 2026